

*Clumping in Hot Star Winds*

W.-R. Hamann, A. Feldmeier & L.M. Oskinova, eds.

Potsdam: Univ.-Verl., 2008

URN: <http://nbn-resolving.de/urn:nbn:de:kobv:517-opus-13981>

# Spectrum formation in clumpy stellar winds

W.-R. Hamann, L.M. Oskinova & A. Feldmeier  
Universität Potsdam, Germany

Modeling expanding atmospheres is a difficult task because of the extreme non-LTE situation, the need to account for complex model atoms, especially for the iron-group elements with their millions of lines, and because of the supersonic expansion. Adequate codes have been developed e.g. by Hillier (CMFGEN), the Munich group (Puls, Pauldrach), and in Potsdam (PoWR code, Hamann et al.). While early work was based on the assumption of a smooth and homogeneous spherical stellar wind, the need to account for clumping became obvious about ten years ago. A relatively simple first-order clumping correction was readily implemented into the model codes. However, its simplifying assumptions are severe. Most importantly, the clumps are taken to be optically thin at all frequencies (“microclumping”). We discuss the consequences of this approximation and describe an approach to account for optically thick clumps (“macroclumping”). First results demonstrate that macroclumping can generally reduce the strength of spectral features, depending on their optical thickness. The recently reported discrepancy between the H $\alpha$  diagnostic and the P V resonance lines in O star spectra can be resolved without decreasing the mass-loss rates, when macroclumping is taken into account.

## 1 Modeling hot-star winds

Adequate stellar atmosphere models are prerequisite to analyze the spectra of early-type stars and to determine their mass-loss rate. The model calculations must account for the supersonic expansion, and for the strong departure from Local Thermodynamical Equilibrium (LTE).

Non-LTE modeling means to solve consistently two sets of equations. For a given source function that depends on the population numbers,  $S(n)$ , the radiation field  $J$  is obtained by solving the transfer equation, symbolically written as a linear mapping  $\mathbf{A}$ :

$$\mathbf{J} = \mathbf{A} \mathbf{S}(n) . \quad (1)$$

The second set of equations describes the statistical equilibrium between the level populations. These equations are linear in  $n$  and must be fulfilled at each spatial point:

$$\vec{n} \cdot \mathbf{P}(\mathbf{J}) = [0, \dots, 0, 1] \quad (2)$$

The transition probabilities in the matrix  $P$  contain frequency integrals over the radiation field,

$$R_{lu} = \int \frac{4\pi}{h\nu} \sigma_{lu}(\nu) J_\nu \, d\nu , \quad (3)$$

thus closing the circle of mutual dependence between radiation field and population numbers. The radiation transfer couples in space, and the radiative transition rates couple in frequency; a solution of the full 3-D problem is therefore extremely demanding, especially since complex model atoms and millions of spectral lines must be taken into account

for realistic models. For the formal solution of the radiative transfer in multi-dimensional geometries, short-characteristic methods are most promising.

The problem becomes even more complex, when time-dependent hydrodynamic modeling is required. The 3-dimensional density and velocity structure must be obtained from solving the hydrodynamic equations, while the full 3-D radiation transfer provides the radiation pressure.

This situation can only be handled with drastical simplifications. For instance, one may reduce the full non-LTE problem to two atomic levels (cf. the Wind3D code: Lobel, these proceedings). The absorption of X-rays by wind clumps may be treated statistically (see Oskinova et al., these proceedings). For the line formation in turbulent media, analytic solutions have been developed by Gail et al. (1980).

In the following section we will describe the treatment of radiative transfer in the approximation of optically thin clumping, and in Sect. 3 we will present a new approach to line transfer with optically thick clumping.

## 2 Clumping in 1st approximation: “microclumping”

Clumping in first approximation is taken into account in all up-to-date stellar wind codes like CMFGEN, PoWR, or WMBasic. The assumption is that the clumps are smaller than the mean free path of the photons for all frequencies. Furthermore, it is assumed that inside the clumps the density is uniform, and enhanced by a factor  $D$  compared to a

smooth model with same mass-loss rate. The volume filling factor of the clumps is  $f_V = D^{-1}$ , because the interclump medium is assumed to be void.

Thanks to the latter assumption, the rate equations have to be solved only for the clump medium, where the density is  $D\rho$  instead of  $\rho$  in the smooth case. In the equation of radiation transfer, we must replace the opacity  $\kappa(\rho)$  and emissivity  $\eta(\rho)$  by

$$\kappa_D = f_V \kappa_C(D\rho) \quad \text{and} \quad \eta_D = f_V \eta_C(D\rho), \quad (4)$$

respectively. The filling factor  $f_V$  appears here, because statistically any given ray is for the fraction  $f_V$  of its path crossing clumps, and for the rest crossing the interclump void.

For processes which are *linear* in density,  $f_V$  and  $D$  cancel out in Eqs. 4. For processes scaling with the *square* of density, however, opacities and emissivities are effectively enhanced by the factor  $D$ .

Line absorption, for instance, scales linearly with  $\rho$ . In contrast, emission lines are typically formed in recombination cascades, and therefore  $\rho^2$ -dependent. In addition, strong emission lines show weak, extended line wings that are due to the frequency redistribution of line photons by electron scattering. (Because of their small mass, electrons have a high thermal speed, e.g.  $v_{\text{th}} = 550$  km/s for  $T_e = 10$  kK.) The electron scattering opacity scales *linearly* with density.

Indeed, homogeneous wind models notoriously predict too strong electron scattering wings for strong WR emission lines (see Fig. 2). When increasing the clumping factor  $D$ , and reducing the mass-loss rate  $\dot{M}$  such that  $\dot{M}\sqrt{D}$  is preserved, the emission lines approximately keep their strength, but the electron-scattering wings are reduced. This effect can be used to determine the clumping factor  $D$ , as pointed out first by Hillier (1991).

For WR stars this method yields typical clumping factors  $D$  between 4 and 10 (e.g. Hamann & Koesterke 1998). For a few [WC]-type Central Stars, Todt et al. (these proceedings) find marginal evidence for the same effect. Unfortunately, the method is not applicable for O stars, since their spectra do not show suitable emission line wings. In this case, only the resonance line absorptions remain as a  $\rho$ -linear diagnostic, especially the unsaturated P V doublet (cf. Sect. 3.2).

Simplicity is the only justification for assuming a universal density contrast  $D$  everywhere in the wind. Puls et al. (2006 and these proceedings) compared  $\rho^2$ -diagnostics from different formation radii ( $H\alpha$ , IR and radio free-free continuum) for OB stars and determined the dependence of clumping on the radial coordinate, i.e.  $D(r)$ . For WN stars, Liermann et al. (these proceedings) compared the radio and line forming region. The agreement with *theoretical predictions* for  $D(r)$  from HD modeling is not yet convincing (e.g. Runacres, these proceedings). Vice versa, the clumping stratification  $D(r)$  strongly affects the HD models (Gräfener, these proceedings).

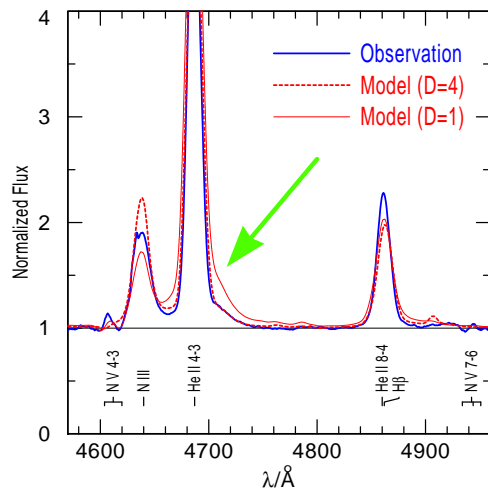


Figure 1: Estimating the microclumping density contrast from electron-scattering line wings, for the WN7 star LMC Brey 24. The observed wing of the He II 4686 line (plotted thick blue) is weaker than calculated with the homogeneous model ( $D=1$ , red thin), but perfectly matched by the clumped model with  $D=4$  (red dashed).

## 3 Macroclumping

### 3.1 X-rays: continuous absorption

According to the widely accepted scenario, X-rays from hot-star winds are produced in shock-heated gas, while the bulk of the stellar wind is in cool clumps which absorb part of the X-rays before they can emerge. The X-rays are mainly emitted in spectral lines, while the absorption is continuous (K-shell photoionization). This decoupling of emission and absorption greatly facilitates a semi-empirical modeling.

Monte-Carlo calculations have been applied to model the emergent X-ray line profiles with randomly distributed line emitters and absorbing clumps (Oskinova et al. 2004, 2006).

Alternatively, one may introduce a statistical treatment that is based on the assumption that the emitting spots and the absorbing clumps are numerous (Feldmeier et al. 2003, Owocki & Cohen 2006). When there are  $n_C$  clumps per unit volume, and each clump is optically thick with a cross section  $\sigma_C$ , the effective opacity becomes

$$\kappa_{\text{eff}} = n_C \sigma_C \quad (5)$$

in full analogy to the usual atomic opacity. If the clumps are not opaque,  $\sigma_C$  is their geometrical cross section diminished by the fraction of transmitted radiation.

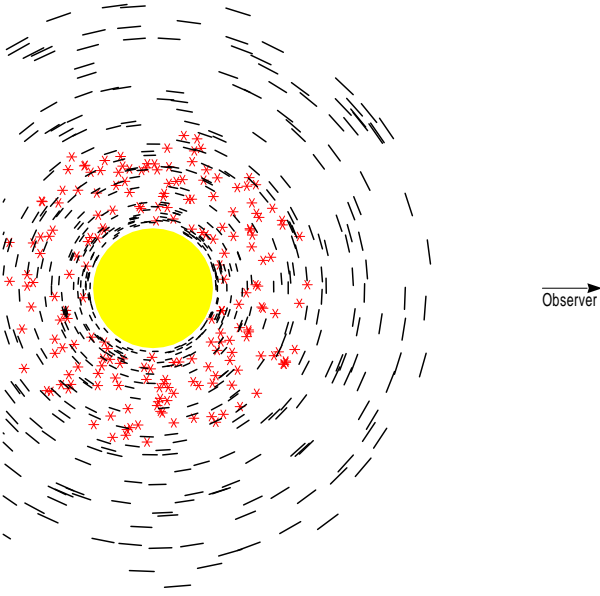


Figure 2: ‘Shell fragment’ model for the formation of X-ray line profiles (Oskinova et al. 2004). Line emission from randomly located spots (red asterisks) is absorbed by shell fragments of continuous opacity.

The Potsdam group (Feldmeier et al. 2003, Oskinova et al. 2004, 2006) found that the observed X-ray line profiles can be explained best if the “clumps” are assumed to have the shape of “pancakes” or “shell fragments” (see Fig. 2). This idea is also supported by the theoretical consideration that the forces which compress the clumps act mainly in radial direction. If clumps are anisotropic, their *projected* cross section must be inserted for  $\sigma_C$  in Eq. (5). This leads to a “venetian blind effect”, where in the limit of entirely flat fragments the opacity scales proportional to  $\mu = \cos \vartheta$  (Fig. 3). With the corresponding effective opacity becoming angle-dependent as  $\kappa_{\text{eff}} \propto \mu$ , the optical depth increment for a ray of any impact parameter growth with the change of radius:  $d\tau \propto |dr|$ , in contrast to the isotropic case where  $d\tau = \kappa dz$ .

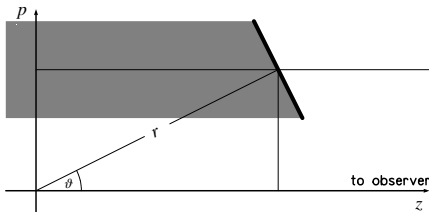


Figure 3: Venetian-blind effect from oriented absorbing slabs. The projected area, and thus the effective opacity, scales with  $\cos \vartheta$ .

### 3.2 Line transfer

The microclumping approximation holds when clumps are small compared to the mean free path of photons. Given the large atomic opacity in many spectral lines, this approximation is not generally justified. It has been relaxed in a recent paper (Oskinova et al. 2007) in favor of a statistical approach to macroclumping in the formal integral of the PoWR stellar-wind code.

It is again assumed that the matter density inside the clumps is enhanced by a factor  $D$  compared to a smooth model with the same mass-loss rate, while the interclump medium is void (clump volume filling factor  $f_V = D^{-1}$ ). For macroclumping, it is now adopted that the clumps have a uniform size with a linear diameter  $\ell$ . Center-to-limb variation of  $\ell$  across a clump is neglected. For this first study, clumps are assumed to be isotropic.

The clumps are statistically distributed with average separation  $L$ . Both  $\ell(r)$  and  $L(r)$  may vary with radial location and are related via the filling factor,

$$f_V = \frac{\ell^3}{L^3} \quad \text{or} \quad D = \frac{L^3}{\ell^3}. \quad (6)$$

The optical depth across one clump of size  $\ell$  is

$$\tau_C = \kappa_C \ell = \kappa_D D \ell, \quad (7)$$

when  $\kappa_C = \kappa(D\rho)$  denotes the opacity of the clump material, and  $\kappa_D = f_V \kappa_C$  the mean opacity in the microclumping approximation (cf. Eq. 4). This can be expressed as

$$\tau_C = \kappa_D L^3 / \ell^2 = \kappa_D h \quad (8)$$

with the definition of the *porosity length*  $h := L^3 / \ell^2$  (Owocki et al. 2004). In terms of the average clump separation  $L$ , the clump optical thickness reads

$$\tau_C = \kappa_D D^{2/3} L \quad (9)$$

The effective absorption cross section of a single clump,  $\sigma_C$ , is its geometrical cross section times the fraction of absorbed photons, i.e.

$$\sigma_C = \ell^2 (1 - e^{-\tau_C}). \quad (10)$$

As the number density of clumps is  $n_C = L^{-3}$ , the effective opacity of the clumpy medium,  $\kappa_{\text{eff}} = n_C \sigma_C$ , becomes

$$\kappa_{\text{eff}} = \frac{\ell^2}{L^3} (1 - e^{-\tau_C}) = h^{-1} (1 - e^{-\tau_C}). \quad (11)$$

As we have  $\tau_C = \kappa_D h$ , this is equivalent to

$$\kappa_{\text{eff}} = \kappa_D \frac{1 - e^{-\tau_C}}{\tau_C}. \quad (12)$$

For optically thin clumps ( $\tau_C \ll 1$ ) the microclumping approximation  $\kappa_{\text{eff}} = \kappa_D$  is recovered. In

the limit of optically thick clumps ( $\tau_C \gg 1$ ) the effective opacity becomes  $\kappa_{\text{eff}} = h^{-1}$ , i.e. the porosity length  $h$  has the meaning of the photon's mean free path. In this limit the effective opacity is reduced by a factor of  $\tau_C$  compared to the microclumping approximation.

In order to evaluate the general opacity reduction factor  $(1 - e^{-\tau_C})/\tau_C$  with the help of Eq. (8), the porosity length  $h(r)$  must be specified. Adopting that the clumping contrast  $D$  can be constrained otherwise, the remaining free parameter is the average clump separation  $L(r)$ .

For the radial dependence of  $L(r)$  we assume that clumps are conserved entities and move radially with  $v(r)$ . Then the number density of clumps obeys an equation of continuity,  $n_C \propto (r^2 v(r))^{-1}$ . As the average separation of clumps is related to  $n_C$  by  $L^3 = n_C^{-1}$ , the radial dependence of  $L(r)$  becomes

$$L(r) = L_0 \left( r^2 \frac{v(r)}{v_\infty} \right)^{1/3}, \quad (13)$$

where the free parameter  $L_0$  describes the typical clump separation in units of the stellar radius.

The total number of clumps that are found at a given instant of time in the radial range between  $r_1$  and  $r_2$  is

$$N_C = \int_{r_1}^{r_2} n_C(r) 4\pi r^2 dr = \frac{4\pi}{L_0^3} (t_2 - t_1), \quad (14)$$

where  $t_2 - t_1$  is the flight time between  $r_1$  and  $r_2$  in units of the dynamical time scale,  $R_*/v_\infty$ . Considering e.g. the radial range from 1.05 to 10.0, and adopting a  $\beta=1$  velocity law, the total number of clumps amounts to  $N_C = 178 L_0^{-3}$ .

Which choice of  $L_0$  is realistic for hot-star winds? The 1-D hydrodynamic simulations by Feldmeier et al. (1997) indicate that one or few radial shells may be launched within one dynamical timescale, which implies that  $L_0 \lesssim 1$  (in units of  $R_*$ ). From *line profile variability* in WR stars, Lépine & Moffatt (1999) conclude that  $\gtrsim 10^4$  clumps are generated per hour, which corresponds to  $L_0 \approx 0.25$ . Our fitting of X-ray line profiles (Oskinova et al. 2006) required  $L_0 \lesssim 1$ .

Now we consider specifically the case of spectral line formation, for which we have to address the issue of Doppler shifts. In our one-component model *the clumps are the wind*. Hence clumps as such move with the wind velocity field  $v(r)$ . In a supersonically expanding medium, rays of a given (observer's frame) frequency can only interact with clumps near the *surface of constant radial velocity* (CRVS). The line opacity of the other clumps is Doppler-shifted out of the resonance. Hence the porosity effect for lines is very pronounced, as illustrated in Fig. 4. Note that even if the "clumps" would have the shape of shell fragments with large cone angle, the CRVS would look porous.

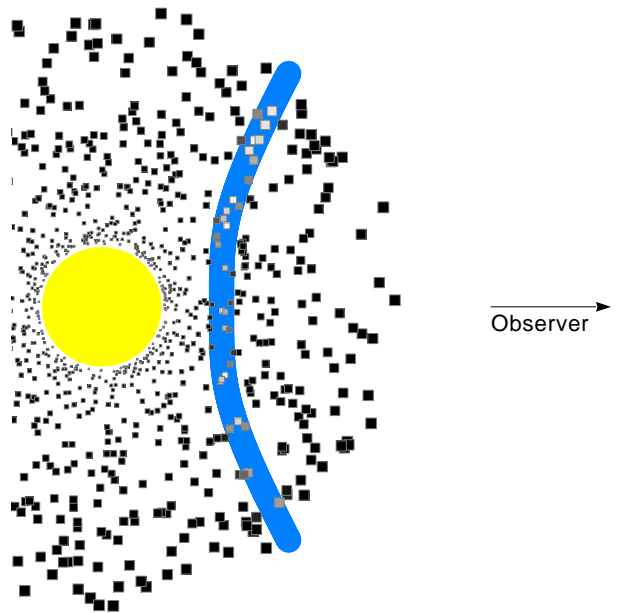


Figure 4: Porosity in the case of line opacity. At a given observer's frame frequency, rays can only interact with those clumps (shaded white or light grey) that are close to the *constant radial velocity surface* (CRVS, blue), while other clumps (black) are out of the line resonance.

Accounting for the finite width of the clump's absorption profile, the CRVS widens to a resonance *zone*. The absorption profile depends on the velocity distribution inside the clump. Broadening can be caused by stochastic motion (thermal, microturbulent), and by velocity gradients, e.g. due to the clump's expansion in radial or lateral direction. For simplicity we adopt that all these effects can be described by a single Gaussian distribution of velocities. Empirically it is known that the narrowest spectral features from stellar winds, like the DACs (discrete absorption components), still have typical widths corresponding to 40 ... 100 km/s. Therefore we evaluate the optical depth across one clump,  $\tau_C$ , as for a *static* medium with a microturbulence velocity  $v_D$  in the mentioned range. Note that the degree of porosity for line radiation depends on this parameter: for smaller  $v_D$ , the opacity profile of a clump profile peaks to a higher maximum, resulting in a smaller effective opacity of the atmosphere.

The described approach to macroclumping has been implemented in the *Potsdam Wolf-Rayet* (PoWR) code. As the only modification, the opacity has been replaced in the *Formal Integral* by the reduced "effective opacity" (Eq. 12). The non-LTE source function is taken from the microclumping model, i.e. the feedback of macroclumping effects on the population numbers is neglected. Al-

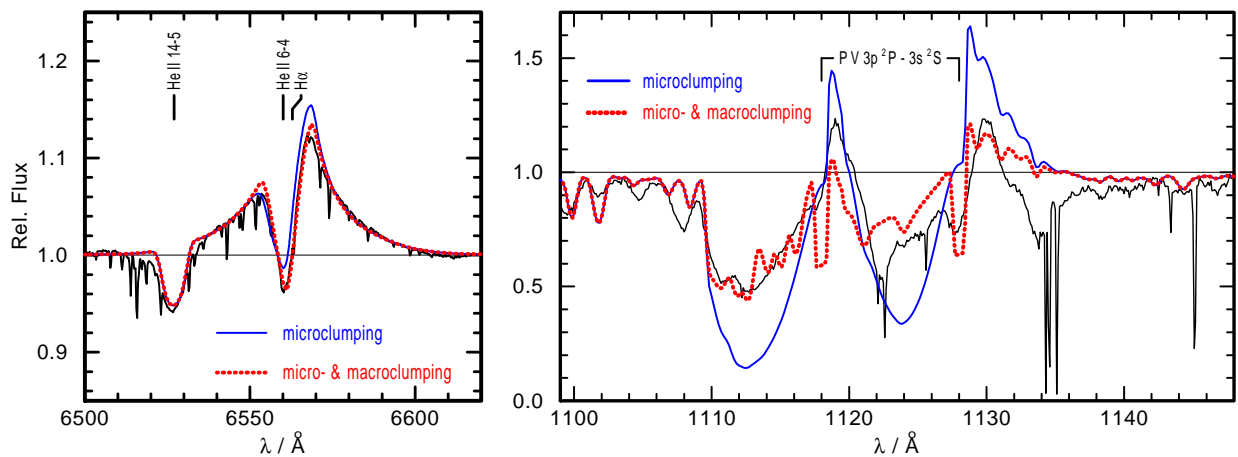


Figure 5: Observed line profiles for  $\zeta$  Puppis (black), compared with synthetic profiles without macroclumping (blue smooth line) and with macroclumping (red dotted). The  $H\alpha$  profile is not affected by macroclumping (left panel). The P V resonance doublet (right panel), however, is predicted much stronger than the observation if neglecting macroclumping, while the model with macroclumping yields a profile of about the observed strength.

though dictated by the need to keep the problem tractable, one can give some justification for this approximation. Most transition rates are not changed by macroclumping, namely all collisional rates, and those radiative transitions for which clumps are optically thin. For those few frequencies where clumps are opaque (i.e. in strong line cores), the average radiation field neglecting macroclumping provides a rough approximation to evaluate the radiative transition rates in the *outer layers* of the clumps. Moreover, the absorption part of the resonance lines from leading ions (e.g. the debated P V line in O stars!) is especially robust against second-order effects on population numbers.

Oskinova et al. (2007) demonstrated the macroclumping effect by means of a model for  $\zeta$  Puppis ( $\log L/L_{\odot} = 5.9$ ,  $\log \dot{M} = -5.56$ ,  $T_* = 39$  kK,  $v_{\infty} = 2250$  km/s,  $v_D = 40$  km/s). For the clumping parameters, a density contrast of  $D = 10$  and an average clump separation parameter  $L_0 = 0.2$  was adopted. The latter gives a reasonable total number of  $2.2 \cdot 10^4$  clumps between  $r = 1.05$  and 10. Clumping assumed to start at the sonic point. As shown in Fig. 5, the effect of macroclumping on  $H\alpha$  is negligible, because this line is not optically thick in the wind. The P V resonance line is predicted much too strong by the model neglecting macroclumping. Its fit would require a ten times smaller  $\dot{M}$  (Fullerton et al. 2006). However, with the macroclumping formalism the model yields the P V line in about the observed strength. Thus macroclumping can resolve the discrepancy between  $\dot{M}$  from resonance line and  $\rho^2$ -diagnostics without decreasing the mass-loss rates.

## 4 Conclusions

*Microclumping* leads to *smaller* empirical mass-loss rates from  $\rho^2$ -diagnostics ( $H\alpha$  line, WR emission lines, radio free-free emission).

*Macroclumping* leads to *higher* empirical mass-loss rates if derived from resonance lines, and is also important for modeling X-ray emission line profiles.

## References

- Castor, J.I., Abbott, D.C., & Klein, R. 1975, ApJ, 195, 157  
 Feldmeier, A., Puls, J., Pauldrach, A.W.A. 1997, A&A, 322, 878  
 Feldmeier, A., Oskinova, L. M., & Hamann, W.-R. 2003, A&A, 403, 217  
 Fullerton, A. W., Massa, D. L., & Prinja, R. K. 2006, ApJ, 637, 1025  
 Gail, H.P., Hundt, E., Kegel, W.H., et al., 1974, A&A, 32, 65  
 Hamann, W.-R., & Koesterke, L. 1998, A&A, 335, 1003  
 Hillier, D. J. 1991, A&A, 247, 455  
 Lépine, S., & Moffat, A. F. J. 1999, ApJ, 514, 909  
 Oskinova, L. M., Feldmeier, A., & Hamann, W.-R. 2004, A&A, 422, 675  
 Oskinova, L. M., Feldmeier, A., & Hamann, W.-R. 2006, MNRAS, 372, 313  
 Oskinova, L. M., Hamann, W.-R., & Feldmeier, A. 2007, A&A, 476, 1331  
 Owocki, S. P., & Cohen, D. H. 2006, ApJ, 648, 565  
 Owocki, S. P., Gayley, K. G., & Shaviv, N. J. 2006, ApJ, 616, 525  
 Puls, J., Markova, N., Scuderi, S., et al. 2006, A&A, 454, 625